

Structural and electronic properties of RuN/GaN superlattices: a first-principles study

C. Ortega López

*Grupo Avanzado de Materiales y Sistemas Complejos - GAMASCO,
Departamento de Física, Universidad de Córdoba, Montería, Colombia.*

R. González-Hernández

*Grupo de Investigación en Física Aplicada. Departamento de Física,
Universidad del Norte, Barranquilla, Colombia,
e-mail: rhernandezj@uninorte.edu.co*

J. Arbey Rodríguez

*Grupo de Estudio de Materiales - GEMA,
Departamento de Física, Universidad Nacional de Colombia, Bogotá, Colombia.
e-mail: jarodriguezm@bt.unal.edu.co*

Recibido el 17 de octubre de 2011; aceptado el 5 de diciembre de 2011

In this work, we investigate the structural and electronic properties of RuN/GaN superlattices, using first-principles calculations within density functional theory (DFT) and generalized gradient approximation (GGA). We have employed the full potential linearized augmented plane waves (FP-LAPW) method as implemented in the WIEN2k code. The 1×1 , 1×2 , 1×3 and 1×4 RuN/GaN superlattices are studied in the wurtzite phase, which is the most stable structure of the GaN. In order to determine the best parameters, we have optimized the total energy as a function of: (i) the unit cell volume, (ii) the c/a ratio and (iii) the z -coordinate of Ga and Ru atoms. Lattices constant, bulk moduli, cohesive and formation energies are reported as a function of the period for each RuN/GaN superlattices, and trends are discussed. On the other hand, a study of the density of states show that the superlattices present a metallic behavior. The results suggest that the RuN/GaN superlattices can be used as compounds for the fabrication of semiconductor-metal-semiconductor or semiconductor-metal devices.

Keywords: Superlattices; nitrides; DFT; LAPW.

PACS: 68.65.Cd; 77.84.Bw; 71.15.Mb; 71.15.Ap

1. Introduction

Gallium nitride (GaN) is one of the wide direct band gap semiconductors, which has a broad range of potential applications for optoelectronic and high power electronic devices. Light emitting diodes (LEDs) are a commercial reality due to an intense activity in the recent past years [1]. Its high thermal conductivity also opens new routes in high-temperature and high-power electronic devices [2,3], such as metal-semiconductor field effect transistors (MESFETs), high electron mobility transistors (HEMTs) and heterojunction bipolar transistors (HBTs) [4,5]. Additionally, high Curie temperatures and room-temperature ferromagnetism have been predicted in GaN-doped with transition metal (TM) elements, which in principle opens a door to semiconductor-based spintronic applications [6-8].

The formation of low resistance and thermally stable ohmic contacts is of considerable technological importance for device performance of GaN-based electronics at high temperatures. In a recent experiment [9] effects on electrical and structural properties of Ru and Ru/Au Schottky contact to n-type GaN indicates that the Ru and Ru/Au contact could be a useful scheme for the realization of high-power electronics applications. A theoretical study of the ruthenium adsorption and diffusion on GaN(0001) surface [10], shows that

the Ru-atom is adsorbed at the T4 position and it presents a 0.61 eV surface diffusion energy barrier. In addition, the ruthenium adsorption induces change on the electronic structure of the clean GaN(0001) surface producing a broadening of the bandwidth around of the Fermi level.

Synthesis of platinum-group metals have received increased attention for the last years and new synthesis strategies have been developed [11,12]. As a result, there is now a growing list of novel platinum-group metal nitrides showing very rich structural, chemical and physical properties [13,14]. Recently, Moreno *et al.* [15] synthesized ruthenium nitride (RuN) by reactive pulsed laser ablation and they found that RuN is an ultra hard material with excellent thermal stability, which is interesting for technological applications. Therefore, it would be interesting to carry out a theoretical study of the electronic structure of the Ru/GaN and RuN/GaN superlattices and their potential use in optoelectronic devices and microelectronic applications.

The purpose of this paper is to study the structural and electronic properties of the RuN/GaN superlattices as possible compounds with other interesting physical properties, and their possible applications in the fabrication of Schottky or ohmic contacts. The theoretical study was focused on wurtzite hexagonal phase, which is the technologically most relevant crystal structure of GaN [16]. The paper is divided

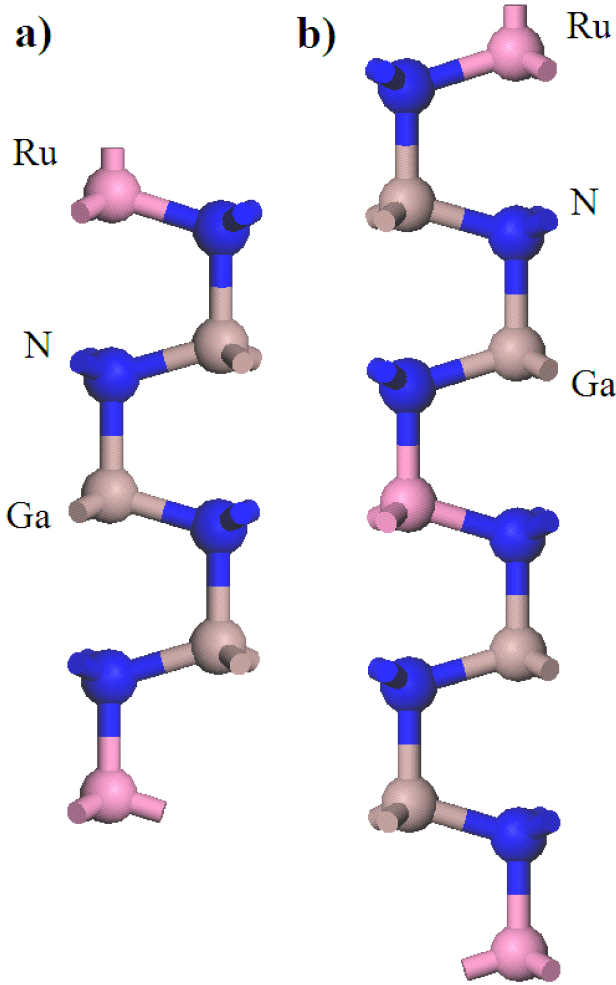


FIGURE 1. (Color online) Side-view of the supercell used to simulate the (a) 1×3 RuN/GaN superlattice which corresponds to the space group C_{6v}^4 , and (b) 1×2 RuN/GaN superlattice which corresponds to the space group C_{3v}^1 . The blue spheres are the N atoms, the gray spheres are the Ga atoms and the pink spheres are the Ru atoms.

as follows: the computational methods will be briefly described in Sec. 2. Section 3 will present results and discussion for the structural and electronic properties of the RuN/GaN superlattices. We will make some concluding remarks in Sec. 4.

2. Methodology

The total energy and electronic structure calculations were performed using an all-electron first principles calculation approach in the framework of the spin density functional theory (DFT). Exchange and correlation effects were treated with generalized gradient approximation (GGA) obtained by Perdew-Burke-Ernzerhof (PBE) [17]. The full-potential linearized augmented plane wave (FP-LAPW) method was employed as implemented in the WIEN2k code [18]. In the LAPW method the unit cell is divided into two types of regions, the atomic spheres centered upon nuclear sites and

the interstitial region between the non-overlapping spheres. Inside the atomic spheres, the wavefunctions are replaced by atomic-like functions, while in the intersphere region the wavefunction of a Bloch state is expanded in planewaves.

The atomic sphere radii used were 1.86, 1.76 and 1.65 a.u. for Ru, Ga and N, respectively. Local orbital extensions were included for the semicore states of the ruthenium atom. The basis set was controlled by a cutoff parameter $R_{mt}k_{max}=8.0$ (where R_{mt} is the smallest atomic sphere radius in the unit cell and k_{max} is a cutoff for the basis function wave vector). The magnitude of the largest vector in charge-density Fourier expansion was $G_{max}=14 \text{ Ry}^{1/2}$. The maximum l values for partial waves inside the spheres and for the non-muffin-tin matrix elements were selected to $l_{max}=10$ and $v_{nmt}=4$, respectively. In order to ensure convergence, we have used 54 nonequivalent k points in the irreducible wedge of the first Brillouin zone for each wurtzite supercell calculations. The integrals over the Brillouin zone were performed using the Monkhorst-Pack (or special-points) method [19]. Self-consistency is achieved by demanding the convergence of the total energy to be smaller than 10^{-5} Ry/cell . The minimization procedure includes the optimization as a function of the volume V and the c/a ratio, followed with the relaxation of the internal atomic coordinates u_i in the optimized values of the lattice parameters. Lattice constants, cohesion energy and bulk modulus were computed by fitting the total energy versus volume, according to the Murnaghan equation of state [20].

The supercell approach is employed to calculate the electronic structure and properties of the short-periodic $1 \times n$ (with $n \leq 4$) RuN/GaN superlattices. In all calculations, we have used a hexagonal wurtzite structure, which is the most stable structure of the GaN. In the supercell construction; two, three and five wurtzite unit cells piled in the [0001] direction for the 1×3 , 1×2 and 1×4 RuN/GaN superlattices were used, respectively. We found that the symmetry of the $1 \times n$ RuN/GaN wurtzite superlattices grown along the symmetry axis depends on the numbers of monolayers n of gallium nitride, in agreement with other reports [21,22]. The appropriate space groups are C_{6v}^4 ($P63mc$) and C_{3v}^1 ($P3m1$) which corresponds to odd and even values of $1 + n$ respectively. The crystal structures of these two different space groups are presented in Fig. 1. In this figure we show the ball and stick model of the 1×3 and 1×2 RuN/GaN superlattices, which are symmetrically equivalent to the 1×1 and 1×4 superlattices respectively.

3. Results and discussions

3.1. Structural properties

To determine the equilibrium geometry of the RuN/GaN superlattices in wurtzite configuration, the independent parameters V (volume of the unit cell), c/a ratio and u_i were optimized as follows: In the first stage, the ideal wurtzite struc-

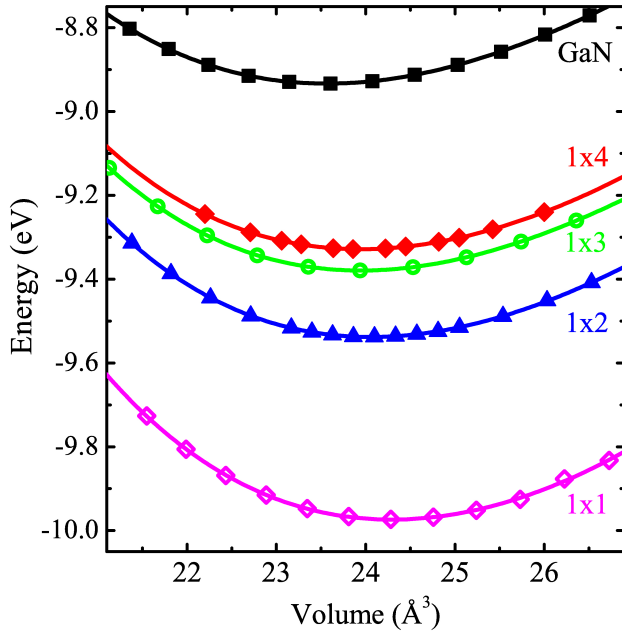


FIGURE 2. (Color online) Energy (eV) versus Volume (\AA^3) of each $1 \times n$ RuN/GaN superlattices in wurtzite structure.

structure was assumed and the equilibrium volume was determined by varying the lattice constant a . After that, the equilibrium volume and u_i were fixed, then energy was optimized as a function of c/a ratio. Again, with c/a ratio and V fixed, u_i were obtained by relaxation of atomic positions using calculated Hellmann-Feynman forces until all the residual force components were less than 0.02 eV/\AA . The new equilibrium volume with c/a ratio and u_i fixed were determined. This procedure was repeated several times until the convergence of the force and energy were reached.

Total energy versus volume data for each $1 \times n$ RuN/GaN superlattices are shown in Fig. 2. Energies and volumes are given per unit formula. From the minimum energy of each superlattices in the Fig. 2, we construct the plot of the cohesion energy versus the period of each RuN/GaN superlattices. We found the minimum energy is increased in a linear tendency when the number of GaN monolayers is increased as it is

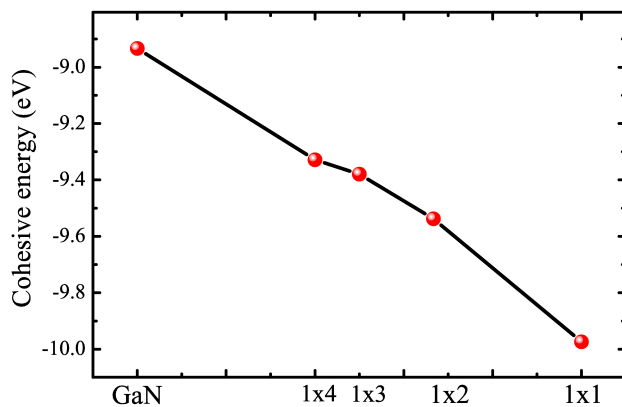


FIGURE 3. Cohesive energy as a function of RuN/GaN superlattice.

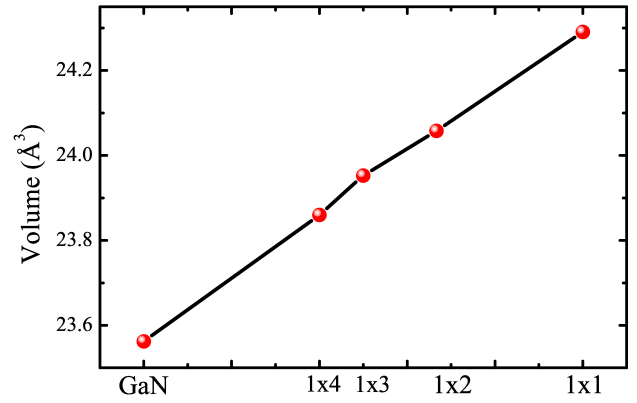


FIGURE 4. Volume (\AA^3) as a function of RuN/GaN superlattice.

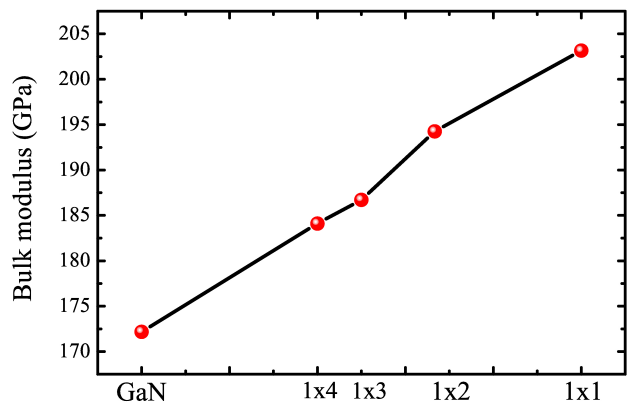


FIGURE 5. Bulk modulus (GPa) as a function of RuN/GaN superlattice.

showed in the Fig. 3. This behavior has been observed in others GaN-based superlattices [23,24].

In the Fig. 4, we observed that equilibrium volume also have a linear tendency with the period of each $1 \times n$ RuN/GaN superlattices. The decreased of RuN/GaN superlattice volume with the increased the number of GaN monolayers can be explained because the RuN monolayer is bigger that the GaN monolayers.

On the other hand, when the number of GaN monolayers increases a uniform decrease of bulk modulus is observed (see Fig. 5). This can be due to the RuN possess a elevated bulk modulus $B_o=335 \text{ GPa}$ [15] in comparison with the value for the GaN, $B_o=173 \text{ GPa}$, in agreement to the experimental value $B_o=188 \pm 40 \text{ GPa}$ [25]. It is seen that the material to be less rigid because the cohesion energy decreases with the number of GaN monolayers is increased.

In the calculations, the total energies are used to calculate the enthalpy of formation and the lattice stability of the RuN/GaN wurtzite superlattices. We have calculated the enthalpy of formation H_f defined as the difference between the total energy of the ternary superlattice $Ru_{1-x}Ga_xN$ phase, $E_{Ru_{1-x}Ga_xN}$, and the reference states of fcc-RuN and w-GaN [26]:

$$H_f = E_{Ru_{1-x}Ga_xN} - (1-x)E_{RuN}^{fcc} - xE_{GaN}^w \quad (1)$$

TABLE I. Calculated structural properties of RuN/GaN superlattices in wurtzite structure. The experimental values are in parentheses [27-29]. Energies and volumes are given per unit formula.

	$a(\text{Å})$	c/a	$V_o(\text{Å}^3)$	$B_o(\text{GPa})$	$E_o(\text{eV})$	$H_f(\text{eV})$
<i>GaN</i>	3.220 (3.189)	1.628 (1.626)	23.56 (22.83)	173 (188±40)	-8.933 (-9.058)	0
1×4	3.239	1.621	23.86	184	-9.328	-0.066
1×3	3.243	1.621	23.95	187	-9.379	-0.035
1×2	3.247	1.622	24.06	194	-9.538	-0.058
1×1	3.255	1.627	24.29	203	-9.974	-0.219

Here, $E_{\text{RuN}}^{\text{fcc}}$ and $E_{\text{GaN}}^{\text{w}}$ are the total energies of fcc-RuN in the rock-salt structure and w-GaN in the wurtzite structure, respectively. The enthalpy of formation estimated for each RuN/GaN superlattices are shown in the Table I. We found a negative value for the enthalpy of formation of the RuN/GaN wurtzite superlattices, which means that they are energetically stable structures with respect to GaN ($H_f^{\text{GaN}} = -1.259$ eV). These results on the structural stability of the RuN/GaN wurtzite superlattices are consistent with earlier experimental results on Ru Schottky contacts to GaN [9].

In the Table I, we summarized the crystal parameters, cohesion energy and enthalpy of formation of the RuN/GaN superlattices and GaN wurtzite calculations. We found that the GaN lattice parameters $a=3.220$ Å and $c/a=1.628$ were slightly overestimated compared to the experimental values $a=3.189$ Å and $c/a=1.626$, respectively [27,28]. These results confirm the usual trend of GGA approach to overestimate the lattice constant values. The internal coordinate $u_i = 0.377$ is in good agreement with the experimental data $u_i=0.377$ for the GaN [29]. The product $u_i \cdot c$ gives the bond length between the cation (Ga or Ru) and the anion (N) sublattices along the z direction. The Ga-N average bond lengths were 2.081, 2.046, 2.023 and 2.014 Å, while the Ru-N bond lengths were 2.135, 2.118, 2.104 and 2.097 Å for the 1×1, 1×2, 1×3 and 1×4 RuN/GaN superlattices respectively. The Ga-N bond lengths are slightly elongated from the calculated for GaN wurtzite ($d=1.976$ Å).

3.2. Electronic properties

In order to study the electronic properties, total and ruthenium projected density of states (DOS) for the GaN, the RuN/GaN superlattices and the RuN in wurtzite structure are shown in Fig. 6. The black-shaded regions show the d -Ru states. Calculations were carried out for both spin polarization. We found that the total DOS for spin up and for spin down polarizations are identical for each superlattices, and the net magnetic moment per cell was always zero. Therefore, we concluded that the RuN/GaN superlattices do not possess magnetic properties. A similar behavior has been reported by R. de Paiva *et al.* for Ru doped GaN in zincblende structure [30]. This suggests that the RuN/GaN superlattices

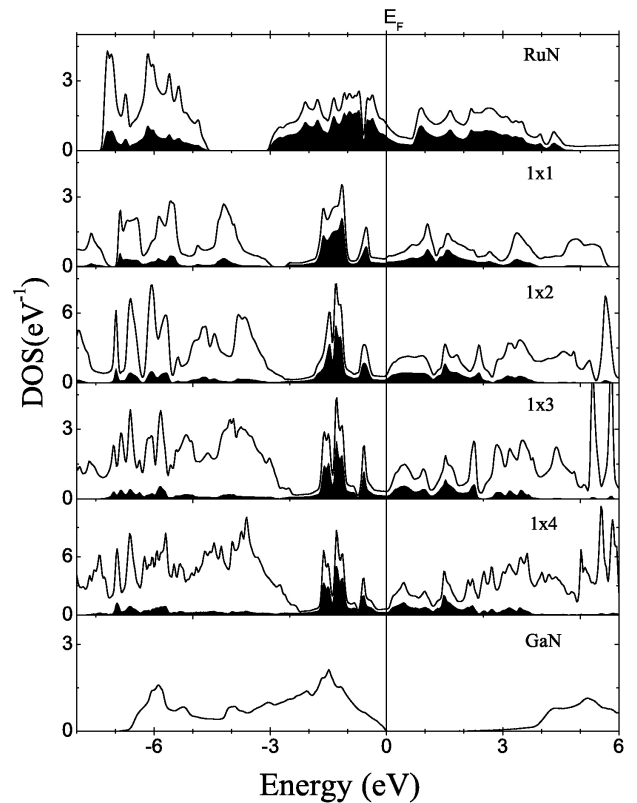


FIGURE 6. Total and partial density of state for the RuN, 1×1, 1×2, 1×3, 1×4 RuN/GaN superlattices and GaN. The black-shaded regions show the d -Ru states. The Fermi energy level is denoted as 0 eV.

are not promising candidates for diluted magnetic semiconductors (DMS) applications.

We can see in the Fig. 6, from top to bottom, that there is gradual transformation of electronic structure as GaN monolayers are introduced in the 1× n RuN/GaN superlattices. It is clear that the RuN and the RuN/GaN superlattices present a metallic behavior, contrary to the GaN which present a semiconductor behavior with a direct band gap of 1.90 eV at the Γ point, which is underestimated compared with experimental band gap [31]. This underestimation is inherent in the formulation of density functional theory and is well documented in existing literature. From the Fig. 6, as the number of GaN monolayers is decreased in the RuN/GaN superlattices, the

impurity d band in the valence band is broadened due to the overlap of d -Ru wave functions and the d -Ru states are extended to the total valence and conduction bands in the RuN. In the RuN and the RuN/GaN superlattices the bands near the Fermi level are mainly contributed by d -ruthenium orbitals and p -nitrogen orbitals. A considerable p - d hybridization between these orbitals is presented in the valence band, a similar electronic behavior was found by Moreno *et al.* for the ruthenium nitride in the rock-salt structure [15].

4. Conclusion

The electronic and structural properties of $1 \times n$ RuN/GaN wurtzite superlattices have been examined by means of the full potential all-electron density functional theory method. We found that the RuN/GaN superlattices are energetically stable in the wurtzite structure and the RuN monolayers can be grown on GaN(0001), in agreement with recent experimental results. We have also found that the RuN/GaN su-

perlattices do not possess magnetic properties and they are not promising candidates for diluted magnetic semiconductor applications. However, due to the considerable contribution of the d -Ru orbitals at Fermi level, the RuN/GaN superlattices exhibit a metallic behavior. So that the RuN/GaN superlattices can be used as compounds for the fabrication of semiconductor-metal-semiconductor or semiconductor-metal devices.

Acknowledgments

We want to thank to Universidad de Cordoba, Universidad del Norte and DIB Universidad Nacional de Colombia for their financial support during the carrying out of this study. We wish to thank Dr. P. Blaha, Institute of Materials Chemistry TU Wien, for special support.

-
1. S. Nakamura and G. Fasol, *The Blue Laser Diode* (Springer, Berlin, 1997).
 2. S. Nakamura, M. Senoh, N. Iwasa, and S. Nagahama, *Appl. Phys. Lett.* **67** (1995) 1868.
 3. H. Bar-Ilan, S. Zamir, O. Katz, B. Meyler, and J. Salzman, *Materials Science and Engineering A* **302** (2001) 14.
 4. R.J. Trew, M.W. Shin and V. Gatto, *Solid-State Electronics* **41** (1997) 1561.
 5. S.J. Pearton, F. Ren, A.P. Zhang and K.P. Lee, *Materials Science and Engineering: R. Reports* **3** (2000) 55.
 6. R. de Paiva, J.L.A. Alves, R.A. Nogueira, J.R. Leite and L.M.R. Scolfaro, *Brazilian Journal of Physics* **34** (2004) 647.
 7. T. Dietl, H. Ohno, F. Matsukura, J. Cibert and D. Ferrand, *Science* **287** (2000) 1019.
 8. T. Jungwirth, J. Sinova, J. Masek, J. Kucera, and A.H. MacDonald, *Rev. Mod. Phys.* **78** (2006) 809.
 9. C.K. Ramesh, V. Rajagopal-Reddy and K.S.R., Kotteswara Rao, *J. Matter Sci: Matter Electron.* **17** (2006) 999.
 10. C. Ortega, W. Lopez and J.A. Rodriguez, *Applied Surface Science* **255** (2009) 3837.
 11. E. Gregoryanz, C. Sanloup, M. Somayazulu, J. Bardo, G. Fiquet, H.K. Mao and R. Hemley, *Nat. Mater.* **3** (2004) 294.
 12. J. Crowhurst, A. Goncharov, B. Sadigh, C. Evans, P. Morrall, J. Ferreira and A.J. Nelson, *Science* **311** (2006) 1275.
 13. J. Uddin and G. Scuseria, *Phys. Rev. B* **72** (2005) 35101.
 14. M.B. Kanoun and S. Goumri-Said, *Physics Letters A* **362** (2007) 73.
 15. M.G. Moreno-Armenta, J. Diaz, A. Martinez-Ruiz, and G. Soto, *J. of Phys. and Chem. Solid.* **68** (2007) 1989.
 16. Q.Z. Xue, Q.K. Xue, R.Z. Bakhtizin, Y. Hasegawa, I.S.T. Tsong, T. Sakurai and T. Ohno, *Phys. Rev. B.* **59** (1999) 12604.
 17. J.P. Perdew, K. Burke and M. Ernzerhof, *Phys. Rev. Lett.* **77** (1996) 3865.
 18. P. Blaha, K. Schwarz, G. Madsen, D. Kvasnicka and J. Luitz, WIEN2k, *An Augmented Plane Wave Plus Local Orbitals Program for Calculating Crystal Properties* (Vienna University of Technology 2009) . ISBN 3-9501031-1-2
 19. H.J. Monkhorst and J.D. Pack, *Phys. Rev.* **13** (1976) 5188.
 20. F.D. Murnaghan, *Proc. Nat. Acad. Sci.* **30** (1944) 244.
 21. Y.E. Kitaev, M.F. Limonov, P. Tronc and G.N. Yushin, *Phys. Rev. B.* **57** (1998) 14209.
 22. A. Lakdja, B. Bouhafs and P. Ruterana, *Computational Materials Science* **33** (2005) 157.
 23. M.G. Moreno-Armenta, L. Mancera, and N. Takeuchi, *Phys. Stat. Sol. (b)* **238** (2003) 127.
 24. R. Gonzalez, W. Lopez, and J.A. Rodriguez, *Solid State Communications.* **144** (2007) 109.
 25. H. Schulz and K.H. Thiemann, *Solid State Commun.* **23** (1977) 815.
 26. R.F. Zhang and S. Veprek, *Acta Materialia* **55** (2007) 4615.
 27. A. Zoroddu, F. Bernardini, P. Ruggerone and V. Fiorentini, *Phys. Rev. B* **64** (2001) 045208.
 28. K. Kim, W.R.L. Lambrecht and B. Segall, *Phys. Rev. B.* **53** (1996) 1631.
 29. C. Stamp and C.G.V. de Walle, *Phys. Rev. B.* **59** (1999) 5521.
 30. R. de Paiva, R.A. Nogueira and J.L. Alves, *J. Phys.: Condens. Matter* **18** (2006) 8589.
 31. K. Lawniczak-Jablonska *et al.*, *Phys. Rev. B* **61** (2000) 16623.